Design of Complex Wavelet Pulses Enabling PSK Modulation for UWB Impulse Radio Communications

Limin Yu and Langford B. White
School of Electrical & Electronic Engineering,
The University of Adelaide, SA 5005, Australia
Email: {liminyu, lwhite}@eleceng.adelaide.edu.au

***Abstract*— In this paper, we present the design of complex Ultra-wideband (UWB) pulses which enables the phase-shift keying (PSK) modulation for UWB Impulse Radio (IR) Communications. Two classes of complex UWB pulses are proposed based on complex Gaussian wavelets and complex rational orthogonal wavelets respectively. Formulas in closed form are derived for a full control of the time and frequency properties of the designed UWB pulses. The system characterisation of the complex UWB pulse-based PSK modulation and demodulation is presented.A novel PSK demodulator based on complex wavelet signalling is adopted for its unique robustness against timing jitter. Besides the inherent advantages of PSK modulation which lead to high power efficiency and high data rate, the proposed PSK scheme in the UWB communication context provides a more flexible way to construct new UWB modulation schemes by combining PSK with other basic modulation options such as the pulse amplitude modulation (PAM) and the pulse position modulation (PPM). In addition, based on the derived formulas, the proposed UWB pulse design method also provides a solution to the construction of multiband UWB systems.**

I. Introduction

Ultra-wideband (UWB) technology is known as a promising communication technique for many wireless applications. A UWB system features very short pulses on the order of nanoseconds as the transmission signal and operates at baseband without the involvement of carriers. Based on the Federal Communications Commission (FCC)'s regulation on the UWB spectrum of 3.1 to 10.6 GHz , a UWB pulse has to be carefully designed to conform the FCC spectrum mask. Popular UWB pulses include the 2nd derivative of Gaussian, Rayleigh pulse and orthogonal Hermite pulses [1] [2]. Wavelet-based UWB pulses are also proposed [3], e.g., the pulses based on B-spline wavelets [4].

Based on these real UWB pulses, various modulation methods have been proposed for UWB systems, including the conventional binary and M-ary PAM and PPM, BPSK, OOK [5], as well as many modified modulation methods based on the conventional ones, such as the combined M-ary PAM and PPM [6], combined BPSK and M-ary PPM [7], and M-ary PPM with multiple orthogonal UWB pulses [8]. To address the issues of channel estimation, multiple-access, transmit-reference (TR)-based modulation [9] and time-hopping (TH)/direct sequence (DS) spread spectrum PPM schemes [7] are also proposed for UWB systems. It is worth noting that due to the carrier-less nature of the UWB impulse radio (IR) communication, M-ary PSK modulation schemes are not yet considered for UWB single-band system because it is a modulation method that is closely related to the phase of sinusoidal carriers. Notice that as the antipodal modulation, the BPSK scheme is essentially the 2-ary PAM modulation.

In this paper, we demonstrate that PSK modulation schemes are possible for UWB communications by introducing complex UWB pulses. Two classes of complex UWB pulses are proposed based on complex Gaussian wavelets and complex rational orthogonal wavelets respectively. The designed complex UWB pulses are in accordance with the FCC regulated spectrum for UWB communications. Formulas in closed form are derived for the pulse design. The system characterisation of the complex UWB pulse-based PSK modulation and demodulation is presented. Properties achieved and that are highly desired for UWB communications include high power efficiency, high data rate of the PSK transmission, and unique robustness against timing jitter based on a novel demodulation structure.

The paper is organised as follows. The design of two classes of complex UWB pulses is presented in section II. Section III presents the signal characterisation of UWB PSK communication based on complex UWB pulses. The corresponding receiver design is given together with some simulation results illustrating the demodulation process. Section IV presents the conclusions of this study.

II. Complex UWB pulse design

A. Complex Gaussian wavelet based UWB pulses

We define the complex Gaussian wavelet[1] by

$$p(t) = e^{-j2\pi f_c(\frac{t}{\xi})}\ e^{-(\frac{t}{\xi})^2}, \tag{1}$$

where ξ is the time scaling factor and f_c is the basis wavelet center frequency. Although the Gaussian wavelet has infinite support in both the time domain and the frequency

[1]Note that the definition here is different from that of complex Gaussian wavelets in the Matlab wavelet toolbox and is closer to the definition of Gabor wavelets or complex Morlet wavelets. We denote this definition as complex Gaussian wavelet in the sense that it is based on scaled versions of the modulated complex Gaussian function.

domain, it can be derived that p(t) has an effective support of $[-3.5\xi, 3.5\xi]$ (s) in the time domain and an effective support of $[(f_c+1.5)\xi^{-1}, (f_c-1.5)\xi^{-1}]$ (Hz) in the frequency domain which contains more than 99.99% of the total energy. Therefore, $p(t)$ has a waveform of length $T = 7\xi$ and the bandwidth of $BW = 3\xi^{-1}$. An example of the complex Gaussian wavelet with $f_c = 1$ and $\xi = 1$ is shown in Fig. 1.

Two parameters, ξ and f_c, in the definition (1) control the time and frequency properties of $p(t)$. In accordance with the FCC regulation on the UWB spectrum $[3.1, 10.6]$ (GHz), the two parameters have to be selected carefully to conform the FCC spectrum mark. The constraints on these two parameters are derived as follows:

$$(f_c - 1.5)\xi^{-1} \geq 3.1 \ (GHz) \tag{2}$$
$$(f_c + 1.5)\xi^{-1} \leq 10.6 \ (GHz) \tag{3}$$
$$BW = 3\xi^{-1} < 7.5 \ (GHz) \tag{4}$$
$$T = 7\xi = \sigma \ (ns) \tag{5}$$

where σ is the desirable pulse length in nanosecond for a specific application.

Equations (2) and (4) lead to the lower bound on the value of f_c:

$$f_c \geq lb(f_c) = \frac{3.1}{7.5/3} + 1.5 = 2.74 \ (Hz). \tag{6}$$

The upper bound of f_c can be derived from equations (3) and (5) as

$$f_c \leq ub(f_c) = \frac{10.6\sigma}{7} - 1.5 \ (Hz). \tag{7}$$

From (6) and (7), we see that for the existence of a solution of f_c, there is $lb(f_c) \leq ub(f_c)$. Therefore σ has to satisfy

$$\sigma \geq (2.74 + 1.5)7/10.6 = 2.8 \ (ns). \tag{8}$$

Based on a designed UWB pulse length of σ, $\sigma > 2.8ns$, the 2 parameters for the pulse definition can be determined by

$$\xi = \sigma/7 \ (\times 10^{-9}), \tag{9}$$
$$2.74 = lb(f_c) < f_c < ub(f_c) = \frac{10.6\sigma}{7} - 1.5 \ (Hz) \tag{10}$$

Notice that f_c can be selected from a range of values, therefore the designed UWB pulses are not unique. If the length of the UWB pulse is allowed to be relatively long so that the BW of the pulse is relatively narrow comparing to the FCC regulated 7.5 GHz UWB BW, multiple f_c values can be selected to construct multiple orthogonal UWB pulses which meet the FCC mask. In this case, the interval between the selected f_c has to satisfy

$$\Delta f_c = f_c^{(i+1)} - f_c^{(i)} > 3 \ (Hz), i = 1, \cdots, N, \tag{11}$$

where the number of available orthogonal pulses N is determined by

$$\begin{aligned} N &= \left\lfloor \frac{ub(f_c) - lb(f_c)}{\Delta f_c} + 1 \right\rfloor \\ &\approx \lfloor 0.5\sigma - 0.413 \rfloor, \end{aligned} \tag{12}$$

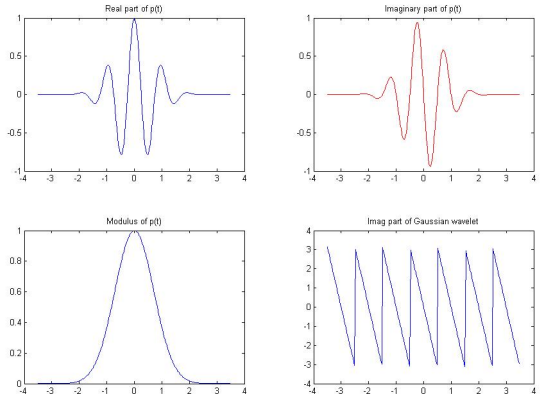

Fig. 1. *Complex Gaussian wavelet with $f_c = 1$ and $\xi = 1$.*

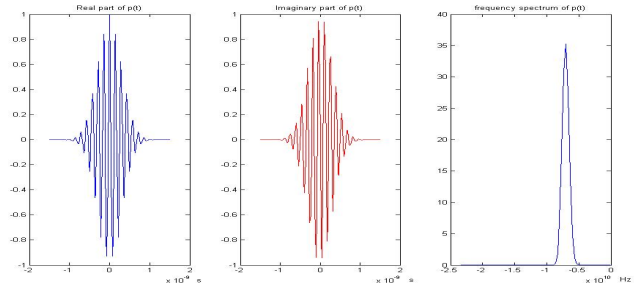

Fig. 2. *a complex Gaussian wavelet-based UWB pulse and its frequency spectrum*

where the operation $\lfloor \cdot \rfloor$ rounds the item $(0.5\sigma - 0.413)$ to the greatest integer less than or equal to its value.

As an example, Fig. 2 shows a complex Gaussian wavelet-based UWB pulse and its frequency spectrum with $\sigma = 3ns$. ξ is around $0.429e-9$. f_c is selected to be 3 Hz from the range of $2.74 < f_c < 3.043$.

B. Complex rational orthogonal wavelet based UWB pulses

In a similar manner, another class of complex wavelets, the complex rational orthogonal wavelets (CROWs) [10], can be designed as UWB pulses in accordance with the FCC regulation for UWB communications. This class of complex wavelets is defined by

$$\psi_+(t) = \psi(t) + j\hat{\psi}(t), \tag{13}$$

where $\psi(t)$ is defined in the frequency domain as

$$\Psi(\omega) = \begin{cases} (2\pi)^{-\frac{1}{2}} e^{j\frac{w}{2}} \sin(\frac{\pi}{2}\beta(\frac{q}{\omega_1}|\omega| - q)), & \omega_1 \leq |\omega| \leq \omega_2 \\ (2\pi)^{-\frac{1}{2}} e^{j\frac{w}{2}} \cos(\frac{\pi}{2}\beta(\frac{q}{\omega_2}|\omega| - q)), & \omega_2 \leq |\omega| \leq \omega_3 \\ 0, & |\omega| \notin [\omega_1, \omega_3], \end{cases} \tag{14}$$

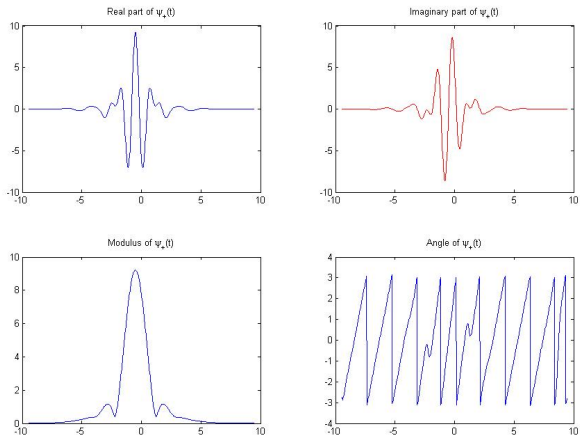

Fig. 3. *Complex rational orthogonal wavelet with $q = 2$ and $\xi = 1$.*

where

$$\begin{aligned} \omega_1 &= (q - \frac{q}{2q+1})\pi \ (rad/s), \\ \omega_2 &= a\omega_1, \\ \omega_3 &= a\omega_2 = a^2\omega_1, \end{aligned} \tag{15}$$

and $q \in Z$. $\beta(t)$ is the construction function which is not unique. One construction function that leads to desirable decay property of the wavelet is given by

$$\beta(t) = t^4(35 - 84t + 70t^2 - 20t^3). \tag{16}$$

$\hat{\psi}(t)$ is the Hilbert transform of $\psi(t)$ and

$$\hat{\Psi}(\omega) = \begin{cases} -j\Psi(\omega), & \omega > 0 \\ j\Psi(\omega), & \omega < 0, \end{cases} \tag{17}$$

The real part and imaginary part of the complex wavelet form a Hilbert transform pair.

The set of wavelets determined by the parameter q, $q \in Z$, are compactly supported in the frequency domain by $[\omega_1, \omega_3]$ with a bandwidth of $\omega_3 - \omega_1 = 2\pi \ (rad/s) = 1 \ (Hz)$, and accordingly have infinite support in the time domain. However, based on the construction function defined in (16), the wavelets have fast decay in the time domain with an effective support of $[-8, 8] \ (s)$. An example of the CROW with $q = 2$ and $\xi = 1$ is shown in Fig. 3.

Defining the UWB pulse as

$$p(t) = \psi_+(t/\xi), \tag{18}$$

where ξ is the time scaling factor, and denoting the bandwidth and pulse length as BW and T respectively, we have the constraints on the pulse design as

$$\omega_1\xi^{-1} \geq 3.1 \ (GHz) \tag{19}$$

$$\omega_3\xi^{-1} \leq 10.6 \ (GHz) \tag{20}$$

$$BW = \xi^{-1} < 7.5 \ (GHz) \tag{21}$$

$$T = 16\xi = \sigma \ (ns). \tag{22}$$

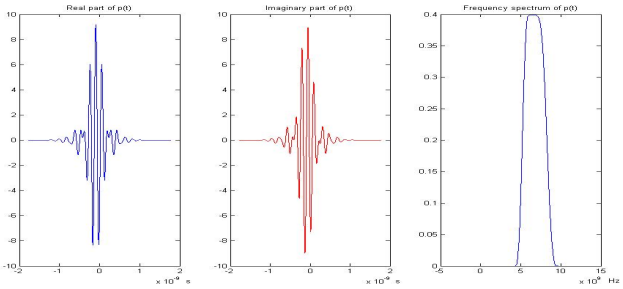

Fig. 4. *a CROW-based UWB pulse and its frequency spectrum*

By substituting (15) into the equations of constraints, the two parameters, q and ξ, can be selected by these constraints. From equations (19) and (21), we have

$$\frac{1}{2}(q - \frac{q}{2q+1}) \geq 3.1/7.5, \ q \in Z, \tag{23}$$

which leads to the lower bound of q as

$$q \geq lb(q) = 2, \ q \in Z. \tag{24}$$

From equations (20) and (22), we have

$$\begin{aligned} & \frac{(q+1)^2}{2q+1} < 10.6\sigma/16 \\ \Rightarrow \quad & q < \frac{2(0.6625\sigma - 1) + \sqrt{(2(0.6625\sigma) - 1)^2 - 1}}{2} \\ & < \frac{2(0.6625\sigma - 1) + 2(0.6625\sigma) - 1}{2} \\ \Rightarrow \quad & q < ub(q) = \frac{2.65\sigma - 3}{2}, \ q \in Z. \end{aligned} \tag{25}$$

For the existence of a solution of q, there is $lb(q) \leq ub(q)$. Therefore σ has to satisfy

$$\begin{aligned} & \frac{2.65\sigma - 3}{2} \geq 2 \\ \Rightarrow \quad & \sigma \geq 7/2.65 \approx 2.64 \ (ns). \end{aligned} \tag{26}$$

Based on a designed UWB pulse length of σ, $\sigma \geq 2.64ns$, the 2 parameters for the pulse definition can be determined by

$$\xi = \sigma/16 \ (\times 10^{-9}), \tag{27}$$

$$2 = lb(q) \leq q < ub(q) = \frac{2.65\sigma - 3}{2}, \ q \in Z. \tag{28}$$

Notice that q can be selected from a set of integers, therefore the designed UWB pulses are not unique. If the length of the UWB pulse σ is allowed to be relatively long, multiple q values can be selected from the range of $[2, \ 2 + (M - 1)]$, where M is the number of available q and is determined by

$$\begin{aligned} M &= \lfloor ub(q) - lb(q) \rfloor \\ &\approx \lfloor 1.325\sigma - 2.5 \rfloor . \end{aligned} \tag{29}$$

For a selected q, multiple orthogonal UWB pulses are available with overlapped frequency spectrum and a dilation factor of

$a = \frac{q+1}{q}$. The number of available orthogonal UWB pulses N can be calculated by

$$\begin{aligned} N &= \left\lfloor \log_a \frac{\omega_1 \xi^{-1}}{3.1} + 1 \right\rfloor \\ &\approx \left\lfloor \frac{\ln \frac{5.161 q^2}{\sigma(2q+1)}}{\ln \frac{q+1}{q}} + 1 \right\rfloor . \end{aligned} \tag{30}$$

Fig. 4 shows a CROW-based UWB pulse and its frequency spectrum with $\sigma = 3ns$. ξ is valued at $0.1875e-9$. q is selected to be 2.

III. M-ARY PSK COMMUNICATION SYSTEM BASED ON COMPLEX UWB PULSES

In this section, we present the system characterisation of UWB PSK communication based on complex UWB pulses. Complex wavelet-based PSK modulation has been presented in [10]. Follow the derivation in [10], the modulated UWB signal and its properties were studied. A novel demodulation method presented in [10] is introduced here. This demodulation method leads to a receiver structure with unique robustness against timing jitter which is a highly desired property for UWB communication systems.

A. M-ary PSK modulation with complex UWB pulses

The transmitted PSK signal are represented as

$$\begin{aligned} s_m(t) &= Re[e^{j\theta_m}\ p(t)],\ m = 1, 2, \cdots, M, \\ &= \cos\theta_m\ p_r(t) - \sin\theta_m\ p_i(t), \end{aligned} \tag{31}$$

where $\theta_m = \frac{2\pi}{M}(m-1) + \theta_0$ and θ_0 is the initial phase coefficient. $p_r(t)$ and $p_i(t)$ are the real and imaginary parts of the complex UWB pulse $p(t)$ respectively. The data sequence is mapped to the phase of the pulse sequence as θ_m. Comparing with the conventional PSK modulation [11], we see that the sinusoidal carrier signal with pulse shaping is replaced by the complex pulse. The transmitted signal is a linear combination of two orthogonal wavelets $p_r(t)$ and $p_i(t)$ in contrast to the conventional orthogonal sine and cosine carriers.

Using the UWB pulse shown in Fig. 2, the signal waveforms of a 4-PSK modulation are shown in Fig. 5. The initial phase θ_0 is $\frac{\pi}{4}$.

B. The receiver design

As shown in [10], a novel receiver structure is applicable based on the complex wavelet signalling, in this case, the complex wavelet pulse UWB signalling. The receiver structure is shown in Fig. 6 and Fig. 7 with complex signal and real signal flow respectively. Follow the derivation in [10], the in-phase and quadrature outputs of the demodulator before sampling, $r_c(t)$ and $r_s(t)$, can be expressed as

$$\begin{aligned} r_c(t) &= \cos\theta_m u(t) + n_c(t), \\ r_s(t) &= \sin\theta_m u(t) + n_s(t). \end{aligned} \tag{32}$$

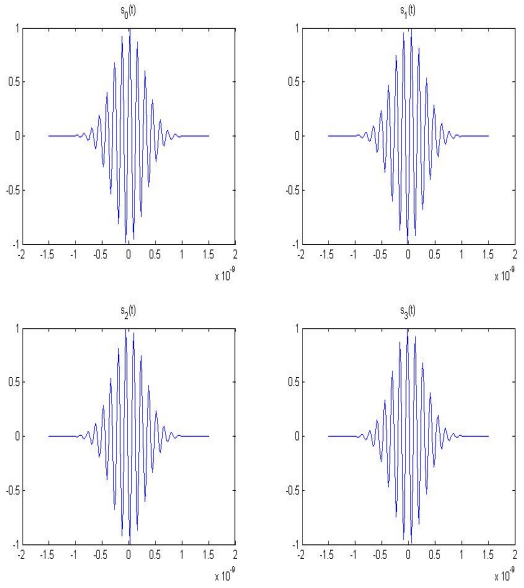

Fig. 5. *Transmitted 4-PSK signal waveforms based on complex Gaussian UWB pulse shown in Fig. 2*

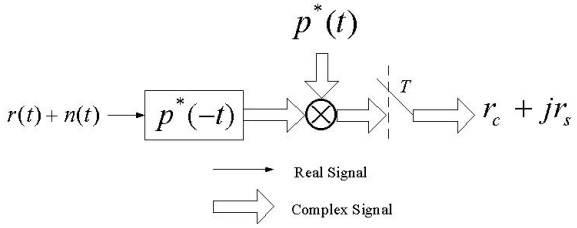

Fig. 6. *PSK demodulation with complex signal flow*

The output decision variables after the periodic sampling are

$$\begin{aligned} r_c &= \cos\theta_m u(T - T_0) + n_c(T - T_0), \\ r_s &= \sin\theta_m u(T - T_0) + n_s(T - T_0), \end{aligned} \tag{33}$$

where T is the symbol period and T_0 is a fixed initial time shift for the periodic sampling which can be selected according to the waveforms of $r_c(t)$ and $r_s(t)$. $n_c(t)$ and $n_s(t)$ are the noise items at the output of the demodulator before sampling. $u(t)$ is a lowpass signal related to the signalling pulse with an explicit expression. (Refer to [10] for more details.)

Based on the transmitted signals shown in Fig. 5, the two filters as shown in the receiver structure can be constructed by discretising the continuous waveform of $p(t)$ at the Nyquist rate and are shown in Fig. 8. Both of them have the filter length of 57.

Fig. 9(a) shows the scatterplot of the output signal before sampling with perfect time synchronisation. The corresponding waveforms of $r_c(t)$ and $r_s(t)$ are shown in Fig. 10. As shown in [10], this demodulation structure has the robustness against the timing error as large as 30% of the pulse period comparing to the traditional correlation based demodulator

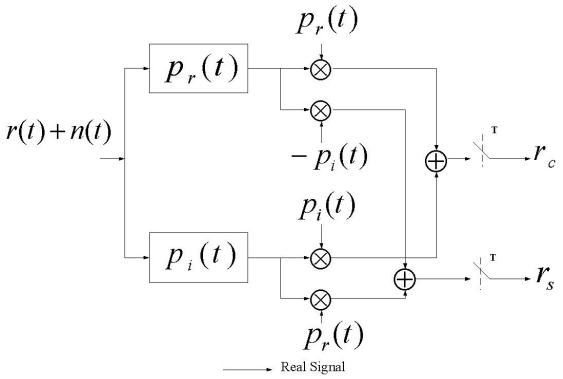

Fig. 7. *PSK demodulation with equivalent real signal flow*

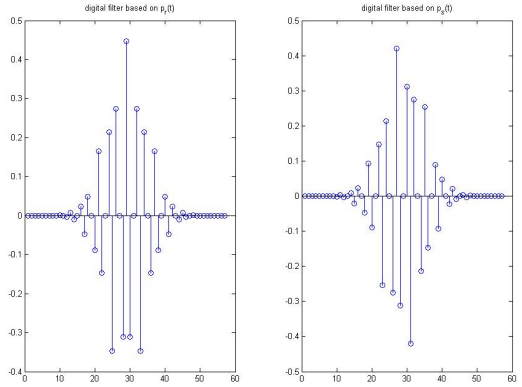

Fig. 8. *two filters at the receiver*

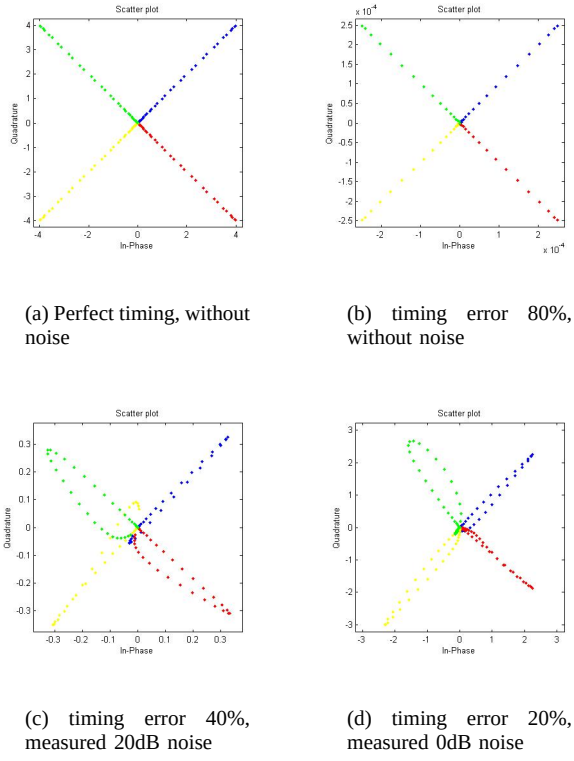

(a) Perfect timing, without noise

(b) timing error 80%, without noise

(c) timing error 40%, measured 20dB noise

(d) timing error 20%, measured 0dB noise

Fig. 9. Scatterplot of the output demodulated signal before sampling

which only works with a timing error less than 1%. For UWB systems, the benefit of this demodulation structure is even more significant because of the relatively long intervals between the pulses. The scatterplot of the output $r_c(t)+jr_s(t)$ with different timing delay errors and an example of the waveforms of $r_c(t)$ and $r_s(t)$ are shown in Fig. 9(b)(c)(d) and Fig. 11. Similar performance is achieved for negative timing delay errors. As shown in Fig. 9(b) and Fig. 11, with a timing delay valued at 80% of the pulse period, the demodulated 4 signal waveforms remain orthogonal but with much smaller amplitudes which makes it very sensitive to noise. In this case, the demodulation performance relies on the signal-to-noise ratio (SNR) of the system which also shows good noise mitigation performance with relatively small but still significant timing error resistance as shown in Fig. 9(d).

IV. Conclusions

In this paper, we present the design of complex UWB pulses which enables PSK modulation for UWB IR Communications. Based on the derived formulas, a number of UWB pulses can be designed with a full control of the time and frequency properties. A novel PSK demodulator based on complex

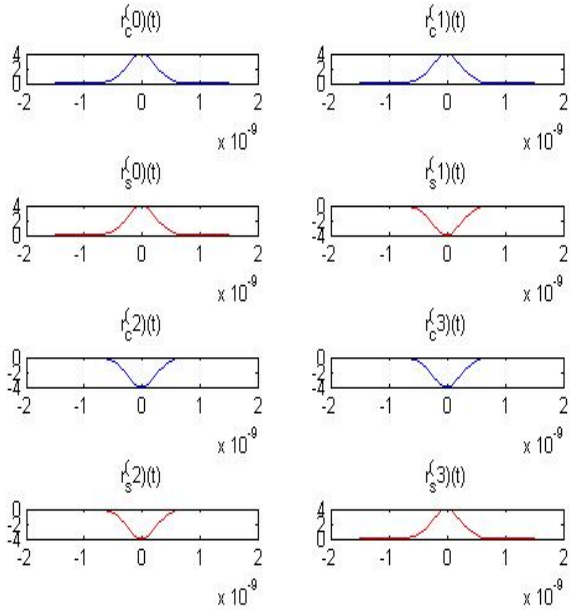

Fig. 10. *Signal waveforms of $r_c(t)$ and $r_s(t)$ for 4-PSK signaling (perfect synchronisation)*

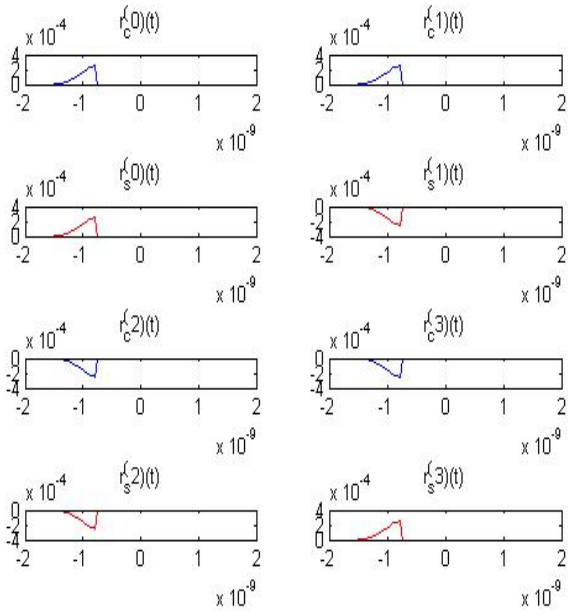

Fig. 11. *Signal waveforms of $r_c(t)$ and $r_s(t)$ for 4-PSK signaling (timing error 80% of the pulse length)*

wavelet signalling can be applied to achieve unique robustness against the timing error. Comparing with other basic modulation schemes, e.g., PAM and PPM, PSK modulation has the inherent advantages of high power efficiency and high data rate under the circumstance of a sufficient SNR level and similar system configurations. More specifically, it provides a more flexible way to construct new modulation schemes, such as combined PSK and PPM modulation and combined PSK, PAM and PPM modulation, which are able to take advantage of the benefits of different modulation schemes and achieve an optimal tradeoff to suit a specific application. The detailed comparison with other modulation options and new combined modulation schemes are to be presented in the consequent paper [12] addressing the analysis on BER performance versus timing jitter and SNR, signal bandwidth efficiency, power efficiency and tradeoffs of the system performance.

The proposed UWB pulse design method also provides a solution to the construction of multiband UWB systems by using relatively long complex UWB pulses (large values of σ). Explicit formulas are derived that indicate the number of subbands available within the FCC mask and the waveforms of the orthogonal subband UWB pulses. Another important fact revealed by this paper is that the CROW-based UWB orthogonal pulses have overlapped spectrum and therefore have better spectrum efficiency than the complex Gaussian wavelet-based UWB pulses. An indication is that with the same pulse length σ, the number of available orthogonal pulses based on CROW is larger than that based on complex Gaussian wavelet as derived in (12) and (30). Based on the work of a new CROW-based OFDM scheme proposed in [13], the extension to the CROW-based Multiband UWB OFDM systems with improved spectrum efficiency and adaptability of the novel demodulator with high timing error resistance is straightforward.

REFERENCES

[1] M. Abdel-Hafez, F. Alaguz, M. Hamalainen, and M. Latva-Aho, "On UWB capacity with respect to different pulse waveforms," *WOCN'05*, pp. 107–111, 2005.

[2] W. Hu and G. Zheng, "Orthogonal hermite pulses used for UWB M-ary communication," *ITCC'05*, vol. 1, pp. 97–101, 2005.

[3] J. Agbinya and H. D. Truong, "UWB signal bandwidth expansion and synthesis using prolate and wavelet functions," *ICMB'05*, pp. 686–689, 2005.

[4] M. Matsuo, M. Kammada, and H. Habuchi, "Design of UWB pulses based on B-splines," *ISCAS'05*, pp. 5425–5428, 2005.

[5] I. Guvenc and H. Arslan, "On the modulation options for UWB systems," *MILCOM'03.*, vol. 2, pp. 892–897, 2005.

[6] H. Zhang, W. Li, and T. A. Gulliver, "Pulse position amplitude modulation for time-hopping multiple-access UWB communications," *IEEE Trans. Comms.*, vol. 53, no. 8, pp. 1269–1273, 2005.

[7] H. Zhang and T. A. Gulliver, "Biorthogonal pulse position modulation for time-hopping multiple access UWB communications," *IEEE Trans. SP.*, vol. 4, no. 3, pp. 1154–1162, 2005.

[8] Y. Kim, B. Jang, C. Shin, and B. F. Womark, "Orthogonal pulses for high data rate communications in indoor UWB systems," *IEEE Comms. Letts.*, vol. 9, no. 5, pp. 405–407, 2005.

[9] J. Sumethnapis and K. Araki, "High performance transmission using differential multi-pulse modulation in transmit-reference ultra-wideband (TR-UWB) communications," *WTS'05*, pp. 141–144, 2005.

[10] L. Yu and L. B. White, "A new complex wavelet and its application in communications," *WITSP'2005*, pp. 343–348, 2005.

[11] J.G.Proakis, "Digital communications," *McGraw-Hill, 5th edition*, 2001.

[12] L. Yu and L. B. White, "Performance analysis of complex wavelet pulse-based PSK modulation for UWB IR communications," *Journal paper in preparation*.

[13] ——, "A new OFDM scheme based on complex rational orthogonal wavelets," *Submitted to APCC'06*.